



Star formation in and around young star clusters associated with H_{II} regions

A. K. Pandey*

Aryabhata Research Institute of Observational Sciences, Nainital 263129, India

Abstract. We are pursuing multi-wavelength studies of young star clusters associated with H_{II} regions to understand the star formation scenario. The young stellar objects (YSOs) in these regions were identified using the near/ mid-infrared colours, slitless spectroscopy and X-ray observations. The optical colour-magnitude diagram of the YSOs indicates that the majority of these objects have ages between 1 Myr to 5 Myr, indicating a non-coeval star formation in the clusters. There is evidence for triggered star formation at the periphery of cluster regions.

Keywords : Star: formation: star clusters

1. Introduction

H_{II} regions have been studied quite extensively in recent years on account of their close association with star formation. There seem to be two modes of star formation associated with H_{II} regions depending on the initial density distribution of the natal molecular cloud. One is the cluster mode which gives birth to rich open clusters and the other is the dispersed mode which forms only loose clusters or aggregates of stars. Presumably, the former takes place in centrally condensed, massive clouds, whereas the latter occurs in clumpy, dispersed clouds (Ogura 2006). These clusters/aggregates of stars emerging from their natal clouds can be the laboratories to study some of the fundamental questions of star formation including different mass and age distributions of the stars, and their interaction with their surrounding interstellar environment. Trends in their evolutionary state and spatial distribution may help to distinguish between various star formation scenarios such as spontaneous or triggered star formation. Triggered star formation is a complex process and makes an interesting and important topic of star formation.

*pandey@aries.res.in

It is believed that majority of the stars in the Galaxy form in clusters that may contain massive ($M \geq 10 M_{\odot}$) as well as low mass stars. A massive star has strong impact on the evolution of its parental molecular cloud. As soon as O stars form their strong ultra-violet (UV) radiation photo-ionizes the surrounding gas and develops an expanding HII region, thus dispersing the remaining molecular cloud. However, the UV radiation can also induce triggering of the next generation star formation. Observational evidence for triggered star formation is often inferred from the spatial distribution of young stars and subgroups of OB associations and their age distribution (see e.g. Sharma et al. 2007; Jose et al. 2008; Pandey et al. 2008; Samal et al. 2007).

One of the triggered star formation processes is known as the ‘collect and collapse process’, which was proposed by Elmegreen & Lada (1977). As the HII region expands, the surrounding neutral material is collected between the ionization front and the shock front which precedes the former. With time the layer gets massive and consequently becomes gravitationally unstable and collapses to form stars of the second generation including massive stars. Recent simulations of this process include Hosokawa & Inutsuka (2005, 2006) and Dale et al. (2007). An observational signature of the process is the presence of a dense layer and massive condensations adjacent to an HII region (e.g. Deharveng et al. 2003).

Another process which has been frequently supported by numerical simulations as well as by observations is radiation driven implosion (RDI) of a molecular cloud condensation. In this process a pre-existing dense clump is exposed to the ionizing radiation from massive stars of the previous generation. The head part of the clump collapses due to the high pressure of the ionized gas and the self-gravity, which consequently leads to the formation of next generation stars. Detailed model calculations of the RDI process have been carried out by several authors (e.g. Bertoldi 1989; Lefloch & Lazareff 1995; Lefloch et al. 1997; De Vries et al. 2002; Kessel-Deynet & Burkert 2003; Miao et al. 2006). The signature of the RDI process is the anisotropic density distribution in a relatively small molecular cloud surrounded by a curved ionization/shock front (bright rim). Bright-rimmed clouds (BRCs) are small molecular clouds located near the edges of evolved HII regions and show the above signature. So they are considered to be good laboratories to study the physical processes involved in the RDI process.

To study the star formation scenario in and around young star clusters, we are pursuing multi-wavelength studies of star-forming regions. In this paper I shall discuss recent results of our multi-wavelength studies of four active star forming regions.

2. Data

The optical observations of the regions were obtained using the 104-cm Sampurnanand telescope of ARIES (Nainital, India), 105-cm Schmidt telescope of the Kiso

Observatory (Japan) and 200-cm Himalayan Chandra Telescope (HCT, Hanle, India) (for details see Sharma et al. 2007; Pandey et al. 2008; Samal et al. 2008). The slitless spectra obtained using the Himalayan Faint Object Spectrograph Camera (HFOSC) instrument at the 200-cm HCT were used to identify the emission line stars in the region.

Near infrared (NIR, JHK_s) data for point sources around the cluster region have been obtained from the 2MASS Point Source Catalogue (PSC). Since young stars in star forming regions are often deeply embedded, the observations at mid-infrared (MIR) observations through the *Spitzer Space Telescope* can provide a deeper insight into the embedded YSOs. YSOs occupy distinct regions in the IRAC colour plane according to their nature; this makes MIR two-colour diagram (TCD) a very useful tool for the classification of YSOs. We have used archival MIR data to identify the MIR excess stars (for details see Chauhan et al. 2009, 2011).

3. Description of the regions

NGC 1893, a very young open cluster, is located at the centre of the Aur OB2 association. NGC 1893 can be recognised as an extended region of loosely grouped early-type stars, associated with the HII region IC 410 with two pennant nebulae, Sim 129 and 130 and obscured by several conspicuous dust clouds. NGC 1893 contains at least five O-type stars.

The Sh 2-294 / RCW3 region is a part of Monoceros cloud complex. In the optical it appears like a butterfly with two wings separated by a dark lane. In the centre of the dark lane a B0.5 star, which is the ionising source of the region, is located

BRC 14 is associated with the molecular cloud IC 1848A to its east, which harbours a bright infrared young cluster AFGL 4029 (Deharveng et al. 1997). The optical and NIR study by these authors revealed that AFGL 4029 is an active star formation site. A deeper NIR survey of the BRC 14 region by Matsuyanagi et al. (2006) supports sequential star formation in this region propagating from the west.

HII region NGC 281/Sh2-184 is located at a relatively high Galactic latitude and has the centrally located cluster IC 1590 (Guetter & Turner 1997; Henning et al. 1994). The brightest member of IC 1590 is an O-type Trapezium-like system HD 5005, whose component stars HD 5005ab (unresolved), HD 5005c, and HD 5005d have spectral types of O6.5 V, O8 V, and O9 V, respectively (Walborn 1973; Abt 1986; Guetter & Turner 1997). The NGC 281 region provides an excellent laboratory to study the star formation through the interaction of high mass stars with their surrounding cloud.

The young cluster NGC 1624 is associated with the bright optical HII region Sh2-212 (Sharpless 1959). Deharveng et al. (2008) studied the region using $J = 2 - 1$

lines of ^{12}CO and ^{13}CO and reported a bright and thin semi-circular structure of molecular gas at the rear side of Sh2-212 along with a filamentary structure extending from southeast to northwest. The semi-circular ring itself contains several molecular clumps, the most massive of which contains a massive young stellar object which is the exciting source of the associated ultra-compact HII (UCHII) region. They concluded that Sh2-212 is a good example of massive-star formation triggered via the collect and collapse process.

4. Membership and age determination

To understand star formation in and around young clusters it is necessary to identify stars directly related to them. We selected probable members associated with the clusters using the following criteria.

The spectra of some of pre-main sequence (PMS) stars, specifically classical T-Tauri stars (CTTSs), show emission lines among which usually $\text{H}\alpha$ is the strongest. Therefore, $\text{H}\alpha$ emission stars have been used to identify the PMS stars associated with the star forming regions. Since many of PMS stars also show NIR/ MIR excess caused by circumstellar disks, NIR/ MIR photometric surveys have also emerged as powerful tools to detect low-mass PMS stars. To identify NIR excess stars from the 2MASS PSC, we used NIR $(J - H)/(H - K)$ colour-colour (NIR-CC) diagram. Since YSOs occupy distinct regions in the IRAC colour plane according to their nature, we have also used MIR TCDs to identify the YSOs adopting the approach given by Allen et al. (2004). The details of the procedure can be found in Pandey et al. (2008), Chauhan et al. (2009). The ages of the identified PMS stars were estimated by using the $V, (V - I)$ colour-magnitude diagram (CMD). The details of the methodology are given by Sharma et al. (2007) and Pandey et al. (2008).

5. Star formation in the region

The distribution of YSOs and morphological details of the environment around the cluster containing OB stars can be used to probe the star formation history of the region. Fig. 1 shows the spatial distribution of detected YSOs around BRC 14, NGC 1893 and NGC 281 regions. The distribution of YSOs around NGC 1893 and BRC 14 region shows an aligned distribution from the vicinity of the ionizing source to the direction of bright rim/ nebulae. A more impressive alignment of the Class II sources in the case of BRC 14, detected using the *Spitzer* observations, can be seen in figure 7 of Koenig et al. (2008). A well aligned distribution of the detected YSOs from the vicinity of the ionization source to the south-west direction of the NGC 281 can also be noticed. This spatial distribution of YSOs resembles with that in the case of NGC 1893 and BRC 14.

To study the age sequence we divided the YSOs associated with BRC 14 into

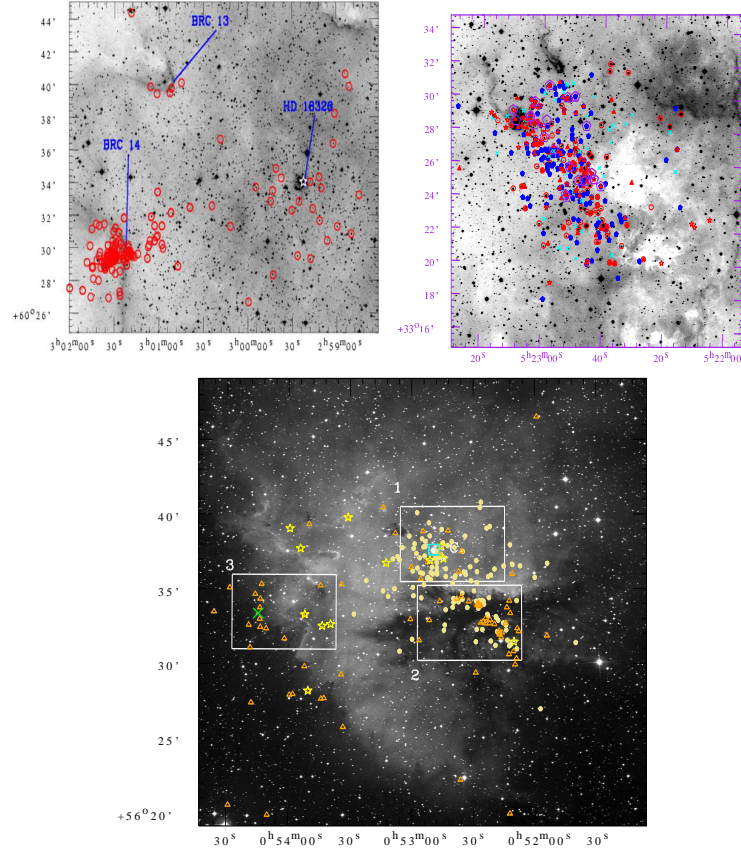


Figure 1. (left): Spatial distribution of YSOs in the BRC 14 and (right): NGC 1893 regions. (bottom): Spatial distribution of YSOs in the NGC 281 region.

two groups: those lying on/inside and outside of the rims (for details see Chauhan et al. 2009). Fig. 2 (left panel) shows the age distribution of these two groups, which manifests that the YSOs lying on/inside the rim (upper panel) are younger than those located outside it (lower panel). A similar trend has been found in the case of several BRCs by Ogura et al. (2007) and Chauhan et al. (2009). The variation of NIR excess $\Delta(H - K)$ and A_V as a function of the distance from the ionization source HD18326 toward BRC 14 is shown in Fig. 2 (right panel), which further indicates that the YSOs located near BRC 14 should be younger than the rest of the stars.

Fig. 3 (left panel: NGC 1893; right panel: NGC 281) shows the age distribution of the YSOs as a function of radial distance from the ionization source of the regions which clearly indicates that the average age of the YSOs located outside the cluster boundary is younger than those of located within the cluster region. The radial variation of the NIR excess $\Delta(H - K)$ in the case of NGC 281, similar to that in the case

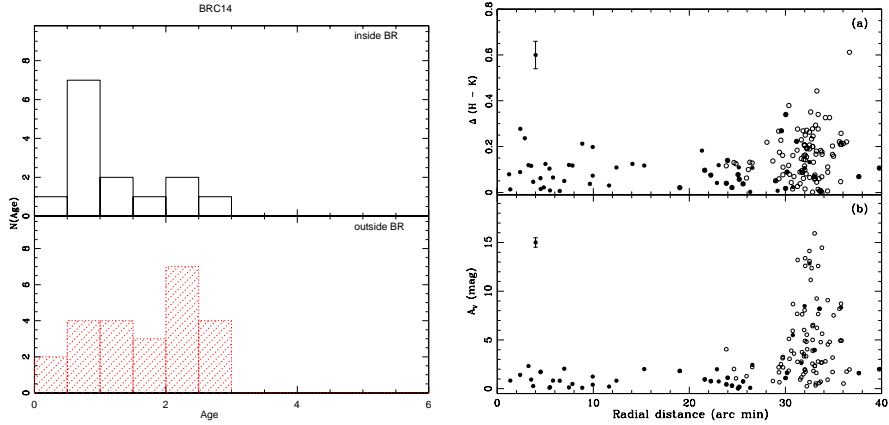


Figure 2. *Left panel:* Age distribution of YSOs in the BRC 14 region lying on/inside (upper) and outside of the rim (lower). *Right panel:* Variation of NIR excess $\Delta(H - K)$ (upper) and A_V (lower) as a function of the distance from the ionization source HD18326.

of BRC14, shows an increasing trend as we move towards the molecular clumps at the periphery of the cluster (cf. Sharma et al. 2012). The youth of the regions outside the cluster boundaries of NGC 1893 and NGC 281 is further supported by the higher fraction of YSOs (40 – 50%) as compared to that in the cluster region (5 – 15%) (cf. Sharma et al. 2007, 2012).

Fig.4 shows JHK_s colour composite image of Sh-294 region from 2MASS data. A close-up view of the colour composite image of Sh-294 region reveals two significant stellar density enhancements in the region. The eastern density enhancement is situated at the border of the main cluster. The contour map of the stellar surface number density around Sh2-294 region is shown in the right panel of Fig.4. The clustering in the central region is obvious in the surface density map. However, several other distinct substructures along with the eastern density enhancement can also be seen. The eastern density enhancement is termed ‘A’ Region. The central region of the Sh-294 contains a B0V star as an ionising source for the region. The probable age of the ionising source is estimated to be ~ 4 Myr, whereas the age of the PMS stars shows spread of 1-5 Myr. The Region ‘A’ is heavily obscured, therefore V and I observations of the regions are not available. However, using the 2MASS NIR JHK data we estimate that $\sim 60\%$ stars in the Region ‘A’ have NIR excess. The fraction of NIR excess stars suggests an age of ≤ 1 Myr for the Region ‘A’.

The age gradient and spatial distribution of YSOs along with the morphology of the ionised gas in the star forming regions discussed above suggest that the star formation activity at the periphery of star clusters is possibly triggered by expansion of HII regions. The morphological features suggest that the triggered star formation may probably be due to the radiation driven implosion.

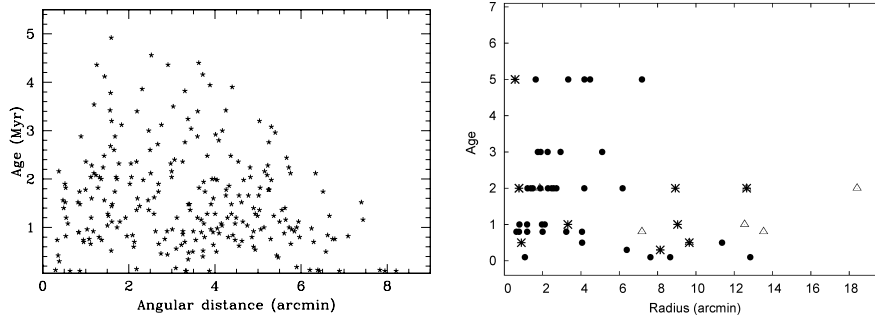


Figure 3. Age distribution of YSOs in the NGC 1893 (*left*) and NGC 281 (*right*) regions.

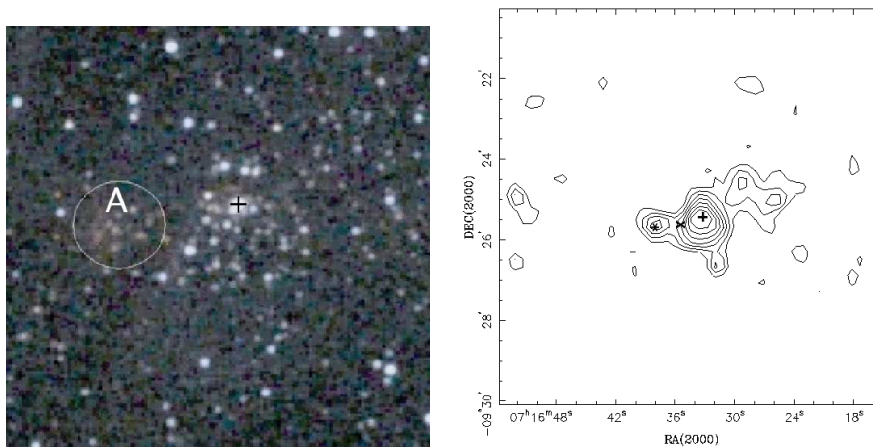


Figure 4. JHK_s colour composite image of Sh-294 region from 2MASS data (*left*) and the contour map of the stellar surface number density around Sh2-294 (*right*).

Fig.5 displays the spatial distribution of YSOs (blue circles; likely Class II sources) in the NGC 1624 region identified on the basis of NIR excess characteristics along with the CO emission contour map from Deharveng et al. (2008) for four condensations and filament. The J drop-out sources are shown using red triangles. The molecular condensations make a semi-circular ring towards the southern side of Sh2-212. Fig.5 reveals that the majority of the YSOs is located close to the cluster centre within a radius of 0.5 arcmin (i.e., within the cluster core radius of ~ 0.9 pc; cf. Jose et al. 2011). However, several other YSOs are found to be distributed outside of this radius along the thin semi-circular ring and filamentary structure. Interestingly, there is an apparent concentration of YSOs just at the boundary of the clump C2. The spatial distribution of sources having $(H - K) \geq 1.0$ mag and J drop-out sources has also been shown in Fig.5 with filled circles and triangles, respectively. Fig.5 reveals a higher density of reddened sources near the clump C2. The larger value of $(H - K)$ (\geq

1.0 mag) could be either due to higher extinction as most of these sources are lying within/very close to the CO distribution, or could be their intrinsic colour due to large NIR excess. Jose et al. (2011) have concluded that the origin of colour excess could be intrinsic in nature. The radial variation of NIR excess, $\Delta(H - K)$, also shows an enhancement in the mean value of $\Delta(H - K)$ near the periphery of the semi-circular ring.

The above facts indicate that the sources near the molecular material are intrinsically redder and support the scenario of possible sequential star formation towards the direction of molecular clumps. The distribution of YSOs in the NGC 1624 region is rather similar to those in other star forming regions. e.g. RCW 82 (Pomarès et al. 2009), RCW 120 (Zavagno et al. 2007) and Sh2-284 (Puga et al. 2009). Majority of the Class I sources in the case of RCW 82 and RCW 120 are found to be associated with the molecular material at their periphery and none are found around the ionizing source. The association of Class I sources with the molecular material manifests the recent star formation at their periphery. If star formation in Sh2-212 region is similar in nature to RCW 82 and RCW 120, one would expect a significant number of Class I sources in the surrounding molecular material of NGC 1624. Unfortunately, the absence of MIR observations hampers the detailed study of the probable young sources lying towards the collected molecular material. However, the YSOs having $(H - K) \geq 1.0$ mag, which are expected to be the youngest sources of the region, are found to be distributed around the molecular clumps detected by Deharveng et al. (2008). It is interesting to mention that in the case of RCW 82, the YSOs having $(H - K) \geq 1.0$ mag are found to be associated with the molecular emission surrounding the H α region. Many of these sources are not observed in the direction of molecular emission peaks, but are located on the borders of the condensations (Pomarès et al. 2009). A similar distribution of YSOs (having $H - K \geq 1.0$) can be seen in the present study at the border of the clump C2.

Deharveng et al. (2008) have concluded that the massive YSO associated with the UCH α region (clump C1) might have formed as a result of the collect and collapse process due to the expansion of the H α region. The model calculation by Deharveng et al. (2008) predicts that the collected layer may get fragmented after 2.2 - 2.8 Myr of the formation of the massive star in Sh2-212. If the sources lying towards the molecular clump C2 and along the filament are formed as a result of the collect and collapse process, these sources must be younger than the ionization source by about 2 - 3 Myr. Since the ionization source is an $O6.5 \pm 0.5$ MS star, the maximum age of the ionization source should be ~ 4 Myr. The present analysis indicates that the sources with $(H - K) \geq 1.0$ seem to have a correlation with the semi-circular ring of molecular condensations and should be younger than the age of the ionization source of the region. However in the absence of optical photometry, the reliable age estimation of these YSOs is not possible. Since the distribution of youngest YSOs on the border of clump C2 has a resemblance to the distribution of Class I/ II YSOs in RCW 82, the formation of these YSOs could be due to the result of small-scale Jeans gravitational instabilities in the collected layer, or interactions of the ionization front

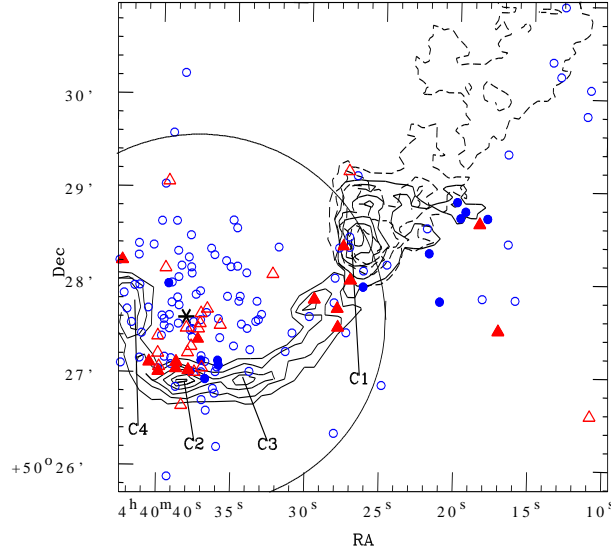


Figure 5. Spatial distribution of YSOs (blue circles in the online version) and the J drop out sources (red triangles). The sources with $(H - K) \geq 1.0$ mag are shown using filled circles and triangles, respectively and the asterisk represents the centre of NGC 1624. The contours represent the $^{13}\text{CO}(2-1)$ emission map from Deharveng et al. (2008) in the velocity range between -34.0 km s^{-1} to -32.7 km s^{-1} (continuous thin contours), -36.1 km s^{-1} to -35.1 km s^{-1} (continuous thick contours) and -36.8 km s^{-1} to -35.9 km s^{-1} (dashed contours), respectively. The partial circle represents the boundary of the cluster.

with the pre-existing condensations as suggested by Pomarès et al. (2009) (for details see Jose et al. 2011).

Acknowledgment

This study is based on recent results of our team work on multi-wavelength studies of star forming regions. I am thankful to Saurabh, Manash, Jessy, Neelam, R. Sagar, W. P. Chen, K. Ogura, B. C. Bhatt, D. K. Ojha and S. K. Ghosh for their contributions.

References

- Abt H. A., 1986, ApJ, 304, 688
 Bertoldi F., 1989, ApJ, 346, 735
 Chauhan N., Pandey A. K., Ogura K. et al., 2009, MNRAS, 396, 964
 Chauhan N., Pandey A. K., Ogura K., Jose J., Ojha D. K., Samal M. R., Mito H., 2011, MNRAS, 415, 1202
 Dale J.E., Bonnell I.A., Whitworth A.P., 2007, MNRAS, 375, 1291

- Deharveng L., Zavagno A., Cruz-Gonzalez I., Salas L., et al., 1997, *A&A*, 317, 459
- Deharveng L., Zavagno A., Salas L., Porras A., et al., 2003, *A&A*, 399, 1135
- Deharveng L., Leoch B., Kurtz S., Nadeau D., Pomares M., Caplan J., Zavagno A., 2008, *A&A*, 482, 585
- Elmegreen B. G., Lada C. J., 1977, *ApJ* 214, 725
- Guetter H. H., Turner D. G., 1997, *AJ*, 113, 2116
- Henning Th., Martin K., Reimann H.-G., Launhardt R., Leisawitz D., Zinnecker H., 1994, *A&A*, 288, 282
- Hosokawa T., Inutsuka S.-I., 2005, *ApJ*, 623, 917
- Hosokawa T., Inutsuka S.-I., 2006, *ApJ*, 646, 240
- Jose J., Pandey A. K., Ogura K., Ojha D. K., et al. 2011, *MNRAS*, 411, 2530
- Jose J., Pandey A. K., Ojha D. K., Ogura K., et al. 2008, *MNRAS*, 384, 1675
- Leoch B., Lazareff B., 1995, *A&A*, 301, 522
- Matsuyanagi I., Itoh Y., Sugitani K., Oasa Y., Mukai T., Tamura M., 2006, *PASJ*, 58, L29
- Miao J., White G. J., Nelson R., Thompson M., Morgan L. 2006, *MNRAS*, 369, 143
- Ogura K., 2006, *BASI*, 34, 111
- Ogura K., Chauhan N., Pandey A. K., Bhatt B. C., Ojha D. K., Itoh Y., 2007, *PASJ*, 59, 199
- Pandey A. K., Sharma S., Ogura K., et al., 2008, *MNRAS*, 383, 1241
- Pomares M., Zavagno A., Deharveng L., Cunningham M., Jones P., Kurtz S., et al., 2009, *A&A*, 494, 987
- Puga E., Hony S., Neiner C., Lenorzer A., Hubert A.-M., et al., 2009, *A&A*, 503, 107
- Samal M. R., Pandey A. K., Ojha D. K., et al., 2007, *ApJ*, 671, 555
- Sharma S., Pandey A. K., Ojha D. K., et al., 2007, *MNRAS* 380, 1141
- Sharma S., Pandey A. K., Pandey J. C., et al., 2012, *PASJ* (in press)
- Zavagno A., Pomares M., Deharveng L., Hosokawa T., Russeil D., Caplan J., 2007, *A&A*, 472, 835